

Non-Drude Optical Conductivity of (III,Mn)V Ferromagnetic Semiconductors

S.-R. Eric Yang,^{1,2} Jairo Sinova,¹ T. Jungwirth,^{1,3} Y.P. Shim,¹ and A.H. MacDonald¹

¹University of Texas at Austin, Physics Department,

1 University Station C1600, Austin TX 78712-0264

²Department of Physics, Korea University, Seoul 136-701, Korea

³Institute of Physics ASCR, Cukrovarnická 10, 162 53 Praha 6, Czech Republic

(Dated: November 21, 2018)

We present a numerical model study of the zero-temperature infrared optical properties of (III,Mn)V diluted magnetic semiconductors. Our calculations demonstrate the importance of treating disorder and interaction effects simultaneously in modelling these materials. We find that the conductivity has no clear Drude peak, that it has a broadened inter-band peak near 220 meV, and that oscillator weight is shifted to higher frequencies by stronger disorder. These results are in good qualitative agreement with recent thin film absorption measurements. We use our numerical findings to discuss the use of f-sum rules evaluated by integrating optical absorption data for accurate carrier-density estimates.

PACS numbers: PACS numbers: 73.20.Dx, 73.20.Mf

I. INTRODUCTION

Recent studies of (III,Mn)V diluted magnetic semiconductors (DMSs), motivated by the discovery of carrier-mediated ferromagnetism [1] in these materials, have uncovered a wealth of interesting phenomenology involving an interplay between collective electronic effects, broken symmetries, interactions, and disorder. The richness of the transport and optical properties of (III,Mn)V DMSs [1, 2] arises from their strong valence-band spin-orbit coupling and from the sensitivity of their magnetic state to growth and annealing conditions, doping, and external fields [3, 4]. *In situ* tunability of material properties by applying gate voltages [5], by illumination [6], or by applying external magnetic fields, suggests many opportunities for exploring new physics or building new devices using these materials. There is considerable evidence that the properties of these systems can be understood using a simplified effective model [7] in which the low energy degrees of freedom are $S = 5/2$ Mn²⁺ local moments, and holes in the host-semiconductor valence band. The Hamiltonian of this effective model should in general include terms that represent scalar and exchange interactions between the Mn ions and the valence band holes, and Coulomb interactions among valence band holes and between the holes and the Mn ions. The simplest theoretical approach to these models, one that appears to be relatively successful in explaining many bulk properties of strongly metallic DMS ferromagnets, either ignores disorder or treats it perturbatively and approximates exchange interactions using a mean-field theory [7, 8, 9, 10] [25]. We have recently presented a theory of the intra-band optical conductivity of (III,Mn)V ferromagnets that uses such an approach [11]. In the present paper we report a finite-size numerical study of the optical conductivity of (Ga,Mn)As in which disorder is treated exactly, enabling us to address weakly metallic or insulating systems and to understand some of the qualitative strong-scattering effects that are omitted in the simpler theory.

Our interest in this property of DMS ferromagnets is motivated by a series of recent optical absorption experiments [12, 13, 14, 15]. The experiments, performed in thin film geometries in both metallic and insulating samples (as judged by the temperature dependence of the resistivity below T_c), exhibit several common features: (a) non-Drude behavior in which the conductivity increases with increasing frequency in the interval between 0 meV and 220 meV, (b) a broad absorption peak near 220–260 meV that becomes stronger as the samples are cooled, and (c) a broad featureless absorption between the peak energy and the effective band gap energy which tends to increase at the higher frequencies. The 220 meV peak can be attributed to inter-valence-band transitions [11], to transitions between the semiconductor valence band states and a Mn induced impurity band, or to a combination of these contributions. Dynamical mean-field-theory studies [16], for a single-band model that neglect the spin-orbit coupling and the heavy-light degeneracy of a III-V semiconductor valence band, demonstrate that non-Drude impurity-band related peaks in the frequency-dependent conductivity occur in DMS ferromagnet models when the strength of exchange interaction coupling is comparable to the valence band width. The conductivities predicted by this model are, however, inconsistent with experiment in temperature trend and appear not to be in the same regime as experimental samples. On the other hand we [11] demonstrated in earlier work that peaks in the conductivity can also occur in the weak-coupling regime, provided that the realistic multi-band character of the valence bands is acknowledged. In this approach the 220 meV peak is due to heavy-hole to light-hole inter-valence-band transitions and the gradual increase in absorption observed in the experiments [13] at frequencies above 500 meV is ascribed to transitions to the bands split-off by strong spin-orbit interactions. Although this theory could account for many overall features of the measured optical conductivity in metallic samples, one prominent feature was at odds with ex-

perimental data, namely the relative magnitudes of the $\omega \rightarrow 0$ conductivity and the 220 meV conductivity peak. The numerical calculations reported on in this paper suggest that this discrepancy is due to multiple-scattering effects that suppress the low-frequency conductivity.

We restrict our attention in this paper to the $T = 0$ limit, which allows us to neglect scattering of valence band quasiparticles off thermal fluctuations in the Mn ion spin orientations. We assume a simple ground state in which the Mn spins have parallel spin orientations [26]. Sources of disorder that are known to have some importance in (III,Mn)V ferromagnets include randomness in the placement of Mn ions on cation sites of the host lattice, random placement of Mn ions at interstitial sites, and randomly located antisite defects in which group V elements are placed at group III element lattice sites. In the low-energy effective model, Mn ions at cation sites have charge $Q = -e$ while interstitial Mn and antisite defects have $Q = 2e$. Coulomb and exchange interactions with the Mn ions have comparable importance [11] for the scattering of valence band holes and must both be included in the theory. In the approach of Ref. 11 these sources of disorder scattering were treated perturbatively using a Born approximation, evaluating the valence band quasiparticle lifetimes using Fermi's Golden rule [17]. In this paper we find the $T = 0$ quasiparticle states for finite-size systems by solving the Schrödinger equation. Unlike the Born approximation theory, this approach does not assume metallic behavior and remains valid at low Mn concentrations when [18] Mn acceptor impurity bands emerge. We find that corrections to the Born approximation theory are important at a quantitative level even for strongly metallic high Mn concentration samples, and that they explain the property that the low-frequency and dc conductivities are suppressed compared to their values in the Born approximation theory. We also find that the f-sum rule, obtained by integrating the conductivity over frequency, differs from its Born approximation value by less than 10% for typical metallic carrier densities.

This paper is organized as follows. Section II defines the model Hamiltonian we use to describe the valence band system in a (III,Mn)V ferromagnet which adds exchange and Coulomb interactions to the six band $\mathbf{k} \cdot \mathbf{p}$ envelope function Hamiltonian of the host (III,V) semiconductor. Section III describes technical issues associated with the evaluation of Kubo linear-response-theory formula for the finite-size system optical conductivity. In Sec. IV we discuss the numerical results we have obtained for different Mn and carrier density regimes, which are in qualitative agreement with experiment and discuss the degree to which aspects of the extreme impurity-band [16] and Golden-rule [11, 17] limits are reflected in the exact results. We also emphasize the feasibility of using the f-sum rule to extract reasonably accurate measurements of the carrier concentration [11], circumventing the inherent uncertainties in Hall measurements in systems with large anomalous Hall effect coefficients.

II. MODEL HAMILTONIAN

We approximate the host semiconductor valence band by its six-band $\mathbf{k} \cdot \mathbf{p}$ Kohn-Luttinger model. This simplification takes advantage of the small number of holes per atom in these ferromagnets. The band electrons interact via Coulomb and exchange interactions with randomly distributed Mn spins and with randomly distributed antisite defects via Coulomb interactions alone; we do not explicitly account for the possible role of Mn interstitials [19]. The requirement of overall charge neutrality implies that the density of valence band holes (p) is related to the density of Mn (n_{Mn}) and the density of antisites (n_{AS}) by $p = n_{Mn} - 2n_{AS}$. In MBE grown (III,Mn)V ferromagnets, it is often a challenge to accurately determine the density of holes, and even the density of Mn ions that have been incorporated into the ferromagnetic state, although progress is being made. It appears at present that any annealing procedure [4, 20] that leads to higher carrier densities, inevitably leads to higher ferromagnetic transition temperatures, and to much higher conductivities [3]. For $\text{Ga}_{0.95}\text{Mn}_{0.05}\text{As}$ for example, it is now possible to prepare samples with $T = 0$ dc conductivities that are close to an order of magnitude larger than in the samples for which ac conductivity measurements have so far been carried out. Although we believe that much of the variability in physical properties can be accounted for in terms of variations in the fraction of Mn ions that are incorporated and, more importantly, variations in the carrier density, it appears likely that a part of this variation is still associated with sources of unintended disorder that are not present in our model. We expect that as unintended disorder is reduced, the properties of these ferromagnets will be more completely determined by the two parameters of our model calculations, p and n_{Mn} [27].

Below we will evaluate the frequency-dependent conductivity by using the Kubo formula description for the linear response of quasiparticles to an electromagnetic field. Coulomb interactions play an essential role in determining the quasiparticle states and interactions among the holes cannot be ignored. In this paper we use a Hartree mean-field approximation for the quasiparticles, which is consistent with the standard bubble diagram approximation we use for the conductivity.

The single particle part of the quasiparticle Hamiltonian may be written as the sum of host crystal band and disorder pieces $\hat{H}^0 = \hat{H}^h + \hat{H}^D$: The disorder Hamiltonian has three contributions $\hat{H}^D = \hat{H}^{K.ex.} + \hat{H}^{Mn-h} + \hat{H}^{As-h}$. \hat{H}^{Mn-h} describes the attractive Coulomb interaction between the ionized Mn^{2+} acceptor and a valence band hole, $\hat{H}^{K.ex.}$ describes the local kinetic-exchange interactions between valence band carriers and the Mn moments, while \hat{H}^{As-h} describes the repulsive Coulomb interaction between a hole carrier and ionized anti-site defects. The single-particle envelope function model Hamiltonian then reads:

$$\hat{H}^0 = \hat{H}^h + \sum_{I=1}^{N_{Mn}} \vec{S}_I \cdot \hat{s} J(\vec{r} - \vec{R}_I) + \sum_{I=1}^{N_{Mn}} \left(-\frac{e^2}{\epsilon|\vec{r} - \vec{R}_I|} - V_0 e^{-|\vec{r} - \vec{R}_I|^2/r_0^2} \right) \hat{I} + \sum_{K=1}^{N_{As}} \frac{2e^2}{\epsilon|\vec{r} - \vec{R}_K|} \hat{I} \quad (1)$$

where $J(\vec{r}) = (J_{pd})/((2\pi a_0^2)^{3/2})e^{-r^2/2a_0^2}$, and $\hat{s} = (\hat{s}_x, \hat{s}_y, \hat{s}_z)$ where $\hat{s}_{x,y,z}$ are the 6×6 matrices which describe hole spins in the representation of the six band envelope-function Hamiltonian, and \hat{I} is a 6×6 unit matrix. In this Hamiltonian, I labels Mn sites, K labels As sites, and \vec{S}_I stands for a Mn spin with quantum number $S = 5/2$. The Mn and As positions are denoted by \vec{R}_I and \vec{R}_K . The term proportional to V_0 is a central cell correction [21] to the Coulomb attraction between holes and Mn acceptors that is known to be required to recover experimental values for the isolated acceptor energy. The quantities N_{Mn} and N_{As} are the number of Mn and As atoms, which we distributed randomly inside cubic simulation cells of side L . Charge neutrality in our simulation cell means that the number of quasiparticle levels occupied by holes is $N_h = N_{Mn} - 2N_{As}$. The values chosen for the phenomenological parameters that appear in this equation are $J_{pd} = 0.05\text{eV nm}^3$, $a_0 = 0.3 \text{ nm}$, $\epsilon = 10.9$, $V_0 = 2.5\text{eV}$ and $r_0 = 0.259 \text{ nm}$.

The host band part of the Hamiltonian is described via the six band Kohn-Luttinger model, with wavevectors \vec{k} in the envelope function replaced by $k_a = \frac{1}{i}\nabla_a$ for $a = x, y, z$ to account for the inhomogeneity induced by disorder. Choosing the angular momentum quantization direction to be along z -axis, and ordering the $j = 3/2$ and $j = 1/2$ basis functions according to the list $(-3/2, 1/2, -1/2, -3/2; 1/2, -1/2)$, the Luttinger Hamiltonian H^L has the form [10]:

$$H^L = \begin{pmatrix} \mathcal{H}_{hh} & -c & -b & 0 & \frac{b}{\sqrt{2}} & c\sqrt{2} \\ -c^* & \mathcal{H}_{lh} & 0 & b & -\frac{b^*\sqrt{3}}{\sqrt{2}} & -d \\ -b^* & 0 & \mathcal{H}_{lh} & -c & d & -\frac{b\sqrt{3}}{\sqrt{2}} \\ 0 & b^* & -c^* & \mathcal{H}_{hh} & -c^*\sqrt{2} & \frac{b^*}{\sqrt{2}} \\ \frac{b^*}{\sqrt{2}} & -\frac{b\sqrt{3}}{\sqrt{2}} & d^* & -c\sqrt{2} & \mathcal{H}_{so} & 0 \\ c^*\sqrt{2} & -d^* & -\frac{b^*\sqrt{3}}{\sqrt{2}} & \frac{b}{\sqrt{2}} & 0 & \mathcal{H}_{so} \end{pmatrix} \quad (2)$$

In the matrix (2) we have highlighted the $j = 3/2$ sector. The Kohn-Luttinger eigenenergies are measured down from the top of the valence band, i.e. they are hole energies. For completeness we list the expressions which define the quantities that appear in H^L :

$$\begin{aligned} \mathcal{H}_{hh} &= \frac{\hbar^2}{2m} [(\gamma_1 + \gamma_2)(k_x^2 + k_y^2) + (\gamma_1 - 2\gamma_2)k_z^2] \\ \mathcal{H}_{lh} &= \frac{\hbar^2}{2m} [(\gamma_1 - \gamma_2)(k_x^2 + k_y^2) + (\gamma_1 + 2\gamma_2)k_z^2] \\ \mathcal{H}_{so} &= \frac{\hbar^2}{2m} \gamma_1 (k_x^2 + k_y^2 + k_z^2) + \Delta_{so} \end{aligned}$$

$$\begin{aligned} b &= \frac{\sqrt{3}\hbar^2}{m} \gamma_3 k_z (k_x - ik_y) \\ c &= \frac{\sqrt{3}\hbar^2}{2m} [\gamma_2 (k_x^2 - k_y^2) - 2i\gamma_3 k_x k_y] \\ d &= -\frac{\sqrt{2}\hbar^2}{2m} \gamma_2 [2k_z^2 - (k_x^2 + k_y^2)]. \end{aligned} \quad (3)$$

with $\gamma_1 = 6.98$, $\gamma_2 = 2.06$ and $\gamma_3 = 2.93$.

The Hartree potential due to interactions among holes must also be included in the single-particle Hamiltonian for quasiparticle states since it captures the screening of Coulomb interactions with impurities due to the build up or depletion of charge. The total one-particle Hamiltonian is $\hat{H} = \hat{H}^0 + \hat{V}^H$, where

$$V_{\vec{k}j, \vec{k}'j'}^H = \delta_{j,j'} \sum_{j''} \sum_{\vec{p}} \frac{4\pi e^2}{\epsilon|\vec{k} - \vec{k}'|^2} \rho_{\vec{p}j'', \vec{k}' + \vec{p} + \vec{k}j''}, \quad (4)$$

and the density matrix

$$\begin{aligned} \rho_{\vec{k}j, \vec{k}'j'} &= \sum_{\alpha} f_{\alpha} \langle \Psi_{\vec{k}j} | \alpha \rangle \langle \alpha | \Psi_{\vec{k}'j'} \rangle \\ &= \sum_{\alpha} f_{\alpha} c_{\vec{k}j}^{(\alpha)} c_{\vec{k}'j'}^{(\alpha)*}, \end{aligned} \quad (5)$$

with $f_{\alpha} = 1(0)$ for an occupied (unoccupied) state. Here $\Psi_{\vec{k}j}(\vec{r}) = e^{i\vec{k}\cdot\vec{r}} u_{\vec{k}j}(\vec{r})$, where $u_{\vec{k}j}(\vec{r})$ are the Bloch functions. The Hartree potential must be determined by solving self-consistently for the density matrix. We have diagonalized this Hamiltonian using a plane-wave representation for the envelope functions of \hat{H}^0 and applying periodic boundary conditions in a cube of size L , which limits wavevectors to the discrete set $\vec{k} = (n_x, n_y, n_z)(2\pi/L)$, where n_x, n_y, n_z are integers. For different system sizes we choose different maximum values of $n_{x,y,z}$, denoted by n_m , so that the maximum wavevector k_{max} is held fixed. For the calculations presented here $k_{max} = \pi \text{ nm}^{-1}$.

III. KUBO FORMULA FOR THE OPTICAL CONDUCTIVITY

We evaluate the real part of the frequency dependent conductivity from the Kubo formula expression which relates it to the quasiparticle eigenvectors $|\alpha\rangle$ and eigenvalues E_{α} .

$$\begin{aligned} \sigma_{ab}(\omega) &= \frac{\pi e^2}{m^2 L^3 \omega} \sum_{\alpha, \beta} (f_{\alpha} - f_{\beta}) \langle \alpha | \hat{p}_a | \beta \rangle \langle \beta | \hat{p}_b | \alpha \rangle \\ &\quad \times \delta(\hbar\omega - E_{\beta} + E_{\alpha}). \end{aligned} \quad (6)$$

Matrix elements of the momentum operator, $\hat{p}_a = \frac{\hbar}{i} \nabla_a$ with $a = x, y, z$, are given by

$$\begin{aligned} \langle \alpha | \hat{p}_a | \beta \rangle &= \sum_{j,j'} \sum_{\vec{k},\vec{k}'} c_{\vec{k}j}^{(\alpha)*} c_{\vec{k}'j'}^{(\beta)} \langle \Psi_{\vec{k}j} | \hat{p}_a | \Psi_{\vec{k}'j'} \rangle \\ &= \sum_{\vec{k},j} c_{\vec{k}j}^{(\alpha)*} c_{\vec{k}j}^{(\beta)} \frac{m}{\hbar} \frac{\partial H_{j,j}^L}{\partial k_a}. \end{aligned} \quad (7)$$

At zero temperature and positive ω the difference ($f_\alpha - f_\beta$) restricts α to occupied quasiparticle states and β to empty quasiparticle states. For finite-size systems the real part of the conductivity is more reliably evaluated by broadening the δ function [22]

$$\begin{aligned} C_R^{ab}(\omega) &= \text{Re} \left[\frac{\hbar e^2}{m^2 L^3} \sum_{\alpha,\beta} \frac{f_\alpha - f_\beta}{E_\beta - E_\alpha} \langle \alpha | \hat{p}_a | \beta \rangle \right. \\ &\quad \left. \times \langle \beta | \hat{p}_b | \alpha \rangle \frac{\gamma}{(\hbar\omega - E_\beta + E_\alpha)^2 + \gamma^2} \right], \end{aligned} \quad (8)$$

with the level broadening, γ , being of the order of the mean level spacing $\sim E_F/N_h \sim 1/L^3$. In the thin film limit the real part of the conductivity is proportional to the absorption coefficient in transmission experiments, $\tilde{\alpha}(\omega) = \frac{8\pi \text{Re}[\sigma(\omega)]}{c(1+n)}$ with $n = \sqrt{\epsilon_0}$ being the zero frequency limit index of refraction of the thin film material and ϵ_0 the dimensionless dielectric constant. This formula for $\tilde{\alpha}(\omega)$ is most accurate in the far infrared regime or in the thin film limit since at higher frequencies multiple scattering from the interfaces must be taken into account. This can be easily done using the standard electromagnetic description of light waves propagating through a medium, but the simple proportionality is lost.

IV. RESULTS

A. Optical conductivity of parabolic band with disorder

It is useful for pedagogical purposes to first present frequency-dependent conductivities calculated with this approach for the case where the 6-band Luttinger model is replaced by a parabolic band model with a mass equal to the heavy hole mass of GaAs. In this way we can partially separate the effects of strong disorder on the optical conductivity from the complications associated with the heavy, light, and split-off valence bands. In the calculation all Mn spins point along the z-axis so that spin up and down single-particle Hamiltonians decouple. For each spin the Hamiltonian is identical to that of Eq. 1 except that \hat{H}^L is replaced by the usual kinetic term $-\hbar^2 \nabla^2 / 2m_{hh}$ and the 6×6 identity matrix is replaced by unity. The following parameters were used in the calculation of the conductivity: $p=0.33 \text{ nm}^{-3}$, $n_{Mn} = 1 \text{ nm}^{-3}$ ($x \approx 4.5\%$), $L = 8 \text{ nm}$, and $n_m = 4$. The results pre-

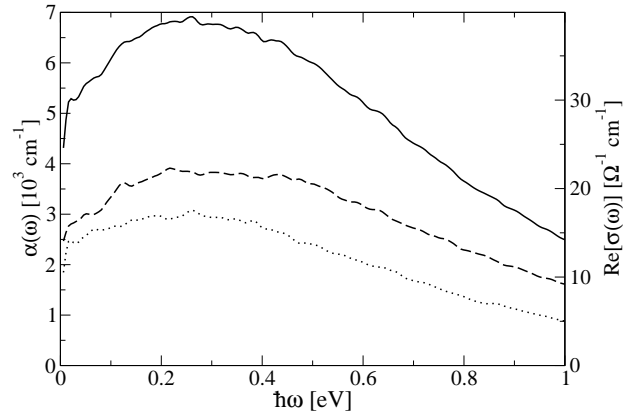


FIG. 1: Absorption and conductivity of minority (dotted line) and majority (dashed line) carriers in a parabolic band approximation. Solid line is the total absorption. Here $p = 0.33 \text{ nm}^{-3}$, $n_{Mn} = 1 \text{ nm}^{-3}$ ($x \approx 4.5\%$).

sented below were obtained by averaging over $N_D = 10$ realizations of the disorder potential.

Fig. 1 shows conductivities and absorption coefficients we have evaluated for minority and majority carriers. Even for this simple band model the conductivity displays clear non-Drude behavior, increasing as a function of frequency at low frequencies. We believe that the non-Drude behavior below 200 meV reflects multiple scattering effects that enhance high-angle scattering and would lead to localization if the disorder were stronger. These effects are explicitly neglected in the Boltzmann transport theory which leads to the Drude formula. The f-sum rule for the conductivity calculated by integrating these numerical results over frequency deviates from the parabolic band model value by less than 10%, demonstrating that the errors induced by constructing a smooth conductivity curve using broadened δ - functions are under reasonable control. The f-sum rule is more accurately satisfied for larger system sizes, for which we are able to choose smaller values of the broadening parameter γ . The non-Drude behavior we find here does capture one aspect of the experimental results. However the overall conductivity magnitude of this model is much smaller than in experiment. Evidently the mixing of heavy and light hole bands leads to quasiparticles with larger velocities.

B. Optical conductivity of Luttinger-Kohn Hamiltonian with disorder

Mixing of heavy- and light-hole bands and its interplay with magnetic order and scattering disorder can be investigated by solving the full Hamiltonian $H = \hat{H}^0 + \hat{V}^H$. This approach treats the band structure realistically and

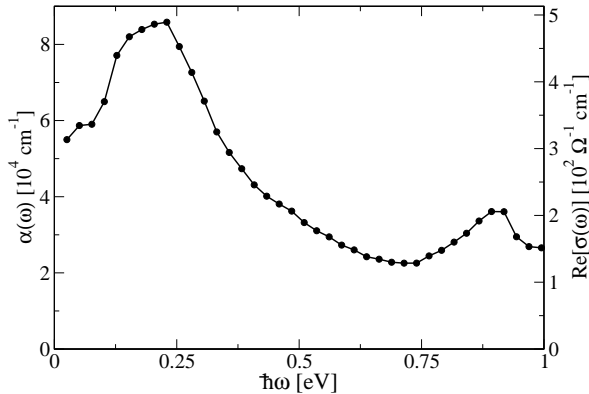


FIG. 2: Absorption and conductivity of a metallic sample computed using a Luttinger Kohn Hamiltonian with disorder. Nominal parameters same as in Fig. 1.

the randomly located charged impurities without approximation. Fig. 2 shows the frequency-dependent conductivity we have evaluated for $p = 0.33 \text{ nm}^{-3}$, $n_{Mn} = 1 \text{ nm}^{-3}$, $L = 6 \text{ nm}$, $N_D = 4$ and $n_m = 3$. For $\hbar\omega < 200 \text{ meV}$ we observe that the conductivity increases with frequency, unlike the Drude formula case. The increase is actually sharper than in the parabolic band model, a property that we believe reflects the additive contributions of non-Drude intra-band absorption and broadened inter-valence-band absorption. There are significant differences between these results and those of the Born approximation (see Fig.1 of Sinova *et al.* [11]) calculated for the same model parameters. In our calculation the maximum value of the absorption is about 90000 cm^{-1} while in the calculation of Sinova *et al.* it is about 110000 cm^{-1} . We believe that this reduction is due to the enhanced backscattering effects captured by the exact calculation and also due to a transfer of spectral weight out of the intra-band contribution. The peak near $\hbar\omega \sim 0.9 \text{ eV}$ in these calculations is due to heavy-hole to split-off band transitions and is more pronounced here than in the Born approximation calculations. The presence of this peak at rather large frequencies emphasizes one weakness of the present calculation, namely that it neglects valence to conduction band transitions. It will be interesting to see whether or not future experiments confirm our prediction of a peak in the absorption due to these transitions that lies at high frequencies, but still clearly below the onset of valence-to-conduction band transitions.

The results shown in Fig. 2 are for parameters that are typical for high T_c (Ga,Mn)As ferromagnets. The dc limits of the conductivities that we calculate are substantially higher than those of the samples for which $\sigma(\omega)$ values have been published at present, but comparable to or smaller than those measured for the highest conductiv-

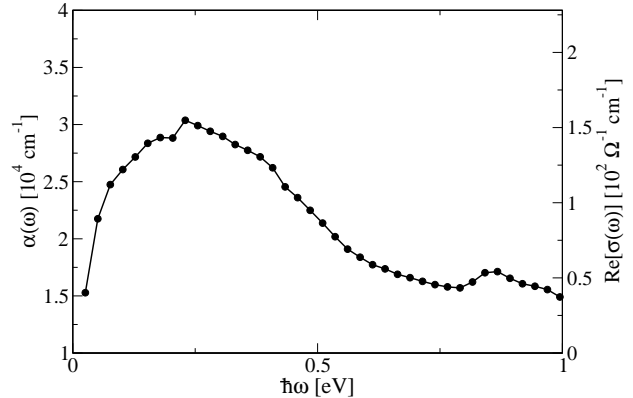


FIG. 3: Absorption and conductivity of a disordered sample computed using a Luttinger Kohn Hamiltonian. The parameters are $p = 0.2 \text{ nm}^{-3}$, $n_{Mn} = 0.88 \text{ nm}^{-3}$, $L = 6 \text{ nm}$, $N_D = 4$ and $n_m = 3$.

ity (Ga,Mn)As ferromagnets currently available. Fig. 3 displays the absorption curves calculated for a more disordered system [28]. The parameters are $p = 0.2 \text{ nm}^{-3}$, $n_{Mn} = 0.88 \text{ nm}^{-3}$, $L = 6 \text{ nm}$, $N_D = 4$ and $n_m = 3$. The conductivity is substantially suppressed at all frequencies, but most strongly at low frequencies. It again has non-Drude behavior at low-frequencies, increasing with increasing frequency over the interval between 0 meV and 220 meV. The broad heavy-to-light absorption peak near 220 meV is still clear but the heavy-hole to split-off band peak is less visible, perhaps explaining the fact that it has not yet been identified experimentally. Hirakawa *et al.* report that the maximum value for absorption in the more disordered sample they study is about 20000 cm^{-1} , which has the same order of magnitude as the value calculated for the parameters of Figure 3.

These results are qualitatively consistent with overall features of the measured optical conductivity, including the overall magnitude [12, 13, 15]. The accuracy of our numerical results is limited somewhat by the wavevector cutoffs that we must invoke in order to make the numerical calculations manageable. This is especially troublesome in estimating the importance of heavy-hole to split-off band transitions. The gradual increase in absorption beyond 500 meV seen in experiment may reflect these transitions. We expect that allowing more wavevectors in our calculations would shift oscillator strength toward higher energies and produce a broader peak, in better agreement with experiments. (Increasing n_m from our current value, 3, by just one changes the dimension of the Hamiltonian matrix from 2058 to 4374, and the resulting self-consistent computation becomes quite substantial.) On the other hand, our investigation of parabolic band case, where n_m can be increased to 4, suggests that system size dependence of low energy non-Drude part of absorption is negligible for n_m bigger than 3.

V. CONCLUSIONS

We have presented a non-perturbative self-consistent study of the optical properties of diluted (III,Mn)V DMS which treats both disorder and interactions on equal footing. Our calculations for the diagonal ac-conductivity are in good qualitative or semi-quantitative agreement with optical absorption experiments in thin film geometries. Several of the non-Drude behaviors observed in the experiments are naturally accounted for in this approach which is able to capture multiple scattering effects that are beyond the scope of perturbative Born approximation approaches [11]. Our calculations show that spin-orbit coupling of valence band holes must be included in the calculation in order to account for the qualitative features of the experiments. It is possible that features associated with heavy-hole to split-off band absorption will emerge more clearly near 0.9 eV when $\sigma(\omega)$ measurements are performed on the most metallic (Ga,Mn)As ferromagnets currently available.

We have used these calculations to test the efficacy of the f-sum rule we proposed in earlier work for carrier density measurements. In applying the f-sum rule to the present system a complication arises, compared to microscopic and parabolic band cases, in that the integrated conductivity depends on the character of the occupied quasiparticle states. In previous work [11] we estimated

that for carrier densities in the range that is interesting for (Ga,Mn)As ferromagnets, the effective mass that should be used in the f-sum rule is $\sim 0.24m_e$, intermediate between heavy and light-hole masses. This estimate was based on calculations of the occupied quasiparticle states that treated disorder perturbatively in the Born approximation. We have found by integrating the optical conductivities evaluated here over frequency that this optical effective mass estimate is reliable at the $\sim 10\%$ level, when disorder is treated exactly. Uncertainties introduced by our finite momentum cut-off do not allow us to estimate the value or the variability of this mass more accurately. Nevertheless, this level of accuracy should be comparable with what is possible from Hall effect measurements which are complicated by the strong anomalous Hall effect in these ferromagnets.

Acknowledgments

This work was supported in part by KOSEF Quantum-functional Semiconductor Research Center at Dongkuk University, the Welch Foundation, DARPA, the Grant Agency of the Czech Republic under grant 202/02/0912, and the Ministry of Education of the Czech Republic under grant OC P5.10.

-
- [1] H. Ohno, H. Munekata, T. Penney, S. von Molnár, , and L. Chang, Phys. Rev. Lett. **68**, 2664 (1992).
 - [2] H. Ohno, A. Shen, F. Matsukura, A. Oiwa, A. Endo, S. Katsumoto, and Y. Iye, Appl. Phys. Lett. **69**, 363 (1996).
 - [3] K. Edmonds, K. Wang, R. Champion, A. Neumann, N. Farley, B. Gallagher, and C. Foxon, cond-mat/0209554.
 - [4] S. J. Potashnik, R. K. C. Ku, Mahendiran, S. H. Chun, R. F. Wang, N. Samarth, and P. Schiffer, cond-mat/0204250.
 - [5] H. Ohno, D. Chiba, F. Matsukura, T. Omiya, E. Abe, T. Dietl, Y. Ohno, and K. Ohtani, Nature **408**, 944 (2000).
 - [6] A. Oiwa, Y. Mitsumori, R. Moriya, T. Supinski, and H. Munekata, Phys. Rev. Lett. **88**, 137202 (2002).
 - [7] J. König, J. Schliemann, T. Jungwirth, and A. H. MacDonald, in *Electronic Structure and Magnetism of Complex Materials*, edited by D. Singh and D. Papaconstantopoulos (Springer Verlag, 2002), e-print [<http://arXiv.org/abs/cond-mat/0111314>].
 - [8] T. Dietl, H. Ohno, F. Matsukura, J. Cibert, , and D. Ferrand, Science **287**, 1019 (2000).
 - [9] T. Dietl, H. Ohno, and F. Matsukura, Phys. Rev. B **63**, 195205 (2001).
 - [10] M. Abolfath, T. Jungwirth, J. Brum, and A. H. MacDonald, Phys. Rev. B **63**, 054418 (2001).
 - [11] J. Sinova, T. Jungwirth, S.-R. E. Yang, J. Kucera, and A. H. MacDonald, Phys. Rev. B **66**, 041202 (2002).
 - [12] Y. Nagai, T. Kunimoto, K. Nagasaka, H. Nojiri, M. Motokawa, F. Matsukura, T. Dietl, and H. Ohno, Jpn. J. Appl. Phys. **40**, 6231 (2001).
 - [13] S. Katsumoto, T. Hayashi, Y. Hashimoto, Y. Iye, Y. Ishiwata, M. Watanabe, R. Eguchi, T. Takeuchi, Y. Harada, S. Shin, et al., Mat. Sci. Eng. B **84**, 88 (2001).
 - [14] K. Hirakawa, private communication.
 - [15] E. Singley, D. Basov, R. Kawakami, , and D. Awschalom, bull. Am. Phys. Soc., [2002 March meeting, Abstract G19.001].
 - [16] E. Hwang, A. Millis, and S. D. Sarma, Phys. Rev. B **65**, 233206 (2002).
 - [17] T. Jungwirth, M. Abolfath, J. Sinova, J. Kucera, and A. H. MacDonald, cond-mat/0206416.
 - [18] S.-R. E. Yang and A. H. MacDonald, cond-mat/0202021.
 - [19] K. M. Yu, W. Walukiewicz, T. Wojtowicz, I. Kuryliszyn, X. Liu, Y. Sasaki, and J. K. Furdyna, Phys. Rev. B. **65**, 201303 (2002).
 - [20] S. J. Potashnik, K. C. Ku, S. H. Chun, J. J. Berry, N. Samarth, and P. Schiffer, con-mat/0105541.
 - [21] A. K. Bhattacharjee and C. B. a la Guillaume, Solid Stat Comm **113**, 17 (2000).
 - [22] J. Imry, *Introduction to Mesoscopic Physics* (Oxford University Press, New York, 1997).
 - [23] G. Zarand and B. Janko, Phys. Rev. Lett. **82**, 047201 (2002).
 - [24] J. Schliemann and A. H. MacDonald, Phys. Rev. Lett. **88**, 137201 (2002).
 - [25] A large database with theory predictions based on this approximation for different host materials, and different carrier and Mn densities can be accessed at

<http://unix12.fzu.ms>.

- [26] The combined effect of disorder and spin-orbit interactions implies that the classical ground state of a (III,Mn)V ferromagnet cannot have perfectly parallel Mn spin orientations. Disorder can also lead to frustration in the carrier-mediated Mn spin interactions, and to complex ground states in which spins are not aligned. Both effects become less important for more strongly metallic (III,Mn)V ferromagnets. See Ref. 23, 24.
- [27] There is a broad consensus that variation in the density of Mn interstitials is responsible for most of the variation of carrier density and magnetically active Mn density that occurs when these materials are annealed. See for example Ref. 19.
- [28] For carrier density drops below $\sim 0.2\text{nm}^{-3}$, disorder localizes the valence band electrons [18]. More strongly localized valence band holes have more heavy-hole character, causing the the optical mass to increase in comparison to values that are appropriate in the metallic limit.